Journal of Quantitative Spectroscopy & Radiative Transfer 306 (2023) 108640

Contents lists available at ScienceDirect

Journal of Quantitative Spectroscopy & Radiative Transfer

journal homepage: www.elsevier.com/locate/jqsrt

The vacuum UV photoabsorption spectrum of 1,1-dibromo-2,2-difluoroethylene (1,1-$Br_2C_2F_2$) in the 5-15 eV photon energy range. Combining experimental and theoretical investigations

R. Locht [a,*], D. Dehareng [b]

[a] MolSys Research Unit, Laboratory for Molecular Dynamics, Department of Chemistry, Institute of Chemistry, Blg.B6c, University of Liège, Sart-Tilman B-4000 Liège 1, Belgium

[b] Centre d'Ingéniérie des Protéines, Institut of Chemistry, Bât.B6a, University of Liège, Sart-Tilman B-4000 Liège 1, Belgium

ARTICLE INFO

Article history:
Received 13 February 2023
Revised 26 April 2023
Accepted 26 April 2023
Available online 2 May 2023

Keywords:
Vacuum UV photoabsorption
Synchrotron radiation
Quantum chemical calculations
Valence and Ryderg transitions
Electronic and vibrational transitions
1,1-dibromo-2,2-difluoroethylene
(1,1-Br2C2F2)

ABSTRACT

Using synchrotron radiation, we have measured the vacuum UV photoabsorption spectrum (PAS) of 1,1-$Br_2C_2F_2$ for the first time between 5 eV and 15 eV photon energy. Quantum chemical calculations have been performed for the determination of excitation and ionization energies. At low energy a weak broad band spreads between 5.2 eV and 6.0 eV and is assigned to $n_{Br}\rightarrow Rp_z$ (3^1B_2) valence transition. A broad continuum starting at 6.18 eV corresponds to the $\pi(3b_1)\rightarrow 5s$ (4^1B_1) Rydberg transition. Starting at E_{exc}^{ad}=6.595 eV a group of four narrower peaks likely corresponds to the vibrational excitation of the characteristic $\pi(3b_1)\rightarrow\pi^*(7^1A_1)$ valence transition. The features evenly spaced by 1315 cm^{-1} are assigned to the C=C stretching vibration. Between 7.0 eV and 11.5 eV, several weak or very strong sharp features are observed. The $3b_1\rightarrow 5p$ Rydberg transition is characterized by a short progression starting at 7.208 eV. A longer progression, assigned to $3b_1\rightarrow 4d$ Rydberg transition, is observed up from 7.932 eV. Both Rydberg states converge to the $\tilde{X}^2B_1$ ionic ground state calculated at IE_{ad}=9.40 eV with quantum defects δ=2.51 and δ=0.96 respectively. The vibrational analysis provides vibrational wavenumbers ω_1=1525±20 cm^{-1}, ω_2=975±40 cm^{-1}, ω_3=620±40 cm^{-1}, ω_4=355±20 cm^{-1} and ω_5=185±30 cm^{-1} averaged over the 5p and 4d Rydberg states. An interaction has likely to be considered between the 6s and 4d Rydberg states. Above 11.5 eV, several strong sharp and broad bands are tentatively assigned to transitions to Rydberg states converging to excited ionic states of 1,1-$Br_2C_2F_2^+$. For one of these a vibrational structure is observed and a tentative assignment is proposed.

1. Introduction

The vacuum UV photoabsorption spectrum (PAS) of the halogenated derivatives of ethylene has often been investigated. However, mainly the mono- and poly-substituted, i.e. chloro-, fluoro- and mixed chloro-fluoro-compounds were considered. Many of these compounds are recognized as potential refrigerant fluids. Recently, the global warming (GWP) and ozone depletion potential (ODP) of numerous halogenated alcanes and alcenes have been evaluated [1].

By far much less attention has been paid to the corresponding bromine derivatives. To the best of our knowledge, no vacuum UV PAS data for 1,1-dibromo-2,2-difluoroethylene (1,1-$Br_2C_2F_2$) are available in the literature. Only infrared and Raman spectroscopic data have been reported by Theimer and Nielsen [2].

In our earlier work, the vacuum UV PAS of C_2H_3Br [3] and 1,1-$Br_2C_2H_2$ [4] have been measured and interpreted. Continuing our investigation on the series of halo-ethylenes, the aim of the present paper is to report on the vacuum UV PAS of 1,1-$Br_2C_2F_2$ recorded for the first time in the 5 eV to 15 eV photon energy range by using synchrotron radiation. To help in the interpretation of the spectrum, quantum chemical calculations applied to this molecule and its cation, will also be presented.

2. Experimental

The experimental setup used in the present work has been described elsewhere [3,5]. Only the most noticeable features will be reported briefly here.

The 3m-NIM monochromator at the 3m-NIM-2 beam line of the BESSY II synchrotron radiation facility (Berlin, Germany) is equipped with an Al/MgF_2 spherical grating of 600 lines/mm. The entrance and exit slits were adjusted at 40 μm and 10 μm re-

* Corresponding author.
E-mail address: robert.locht@uliege.be (R. Locht).

https://doi.org/10.1016/j.jqsrt.2023.108640
0022-4073/

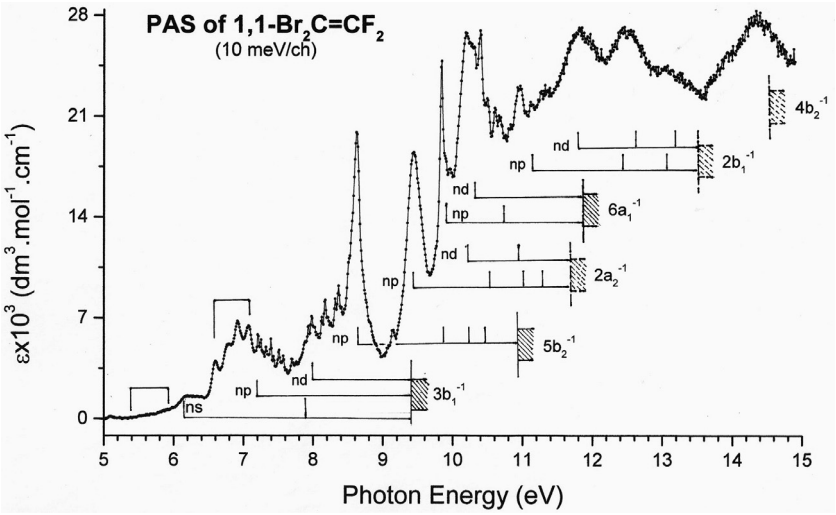

Fig. 1. VUV photoabsorption spectrum of 1,1-$Br_2C_2F_2$ between 5 eV and 15 eV photon energy measured with 10 meV energy increments. Vertical bars and shaded areas locate the Rydberg states converging to ionization continua calculated in the present work and lying below 15 eV.

spectively. In a 30 cm long windowless absorption cell the vapor pressure is measured by a capacitor manometer. The light is detected by a sodium salicylate sensitized photomultiplier. One scan with gas and one with the evacuated absorption cell are required for the recording of an absorption spectrum.

To characterize more easily weak sharp peaks and diffuse structures, often superimposed on a strong continuum, a subtraction procedure could be applied. This method has already been used successfully in previous spectral analyses [5,6]. A severe smoothing of the experimental curve by fast Fourier transform (FFT) simulates the underlying continuum. The result is subtracted from the original photoabsorption spectrum. The resulting diagram will be called Δ-plot in the forthcoming sections. This data handling has been thoroughly investigated and validated by Marmet and Carbonneau [7].

The multiple lines PAS of N_2 between 12 eV and 15 eV [8] has been used to calibrate the monochromator. The accuracy of this calibration is better than 2 meV. The measurements between 5 eV and 11.5 eV have been repeated several times and the PAS has been recorded with energy increments of 0.5 meV and 0.3 meV. The accuracy on the energy position of a feature is estimated to be 2 meV including the calibration error. Above 11.5 eV and up to 15 eV only energy increments of 1 meV have been used and a total error of the same order will be adopted. This evaluation is confirmed by the reproducibility of energy positions measured in different spectra. In the following tables the dispersion will be indicated in parentheses when it exceeds 3 meV.

The commercially available 1,1-$Br_2C_2F_2$, purchased from ABCR and of 97% purity, was used without further purification.

3. Experimental results

The vacuum UV-PAS of 1,1-$Br_2C_2F_2$ as measured between 5 eV and 15 eV photon energy is represented in Fig. 1 by the extinction coefficient ε as a function of the photon energy measured with 10 meV increments. The prominent features are indicated by small vertical bars and shaded areas locate the adiabatic or vertical ionization energies obtained by quantum chemical calculations performed in the present work (see Section 4).

The PAS is clearly divided into three regions: (i) the 5.0-7.0 eV region consisting of a number of weak broad bands and sharper structure superimposed on a continuum, (ii) the 7.0-11.5 eV region containing a large number of weak to very strong sharp features and bands superimposed on a continuum with increasing intensity up from 9 eV to about 10.5 eV and (iii) the region above 10.5 eV and up to 15 eV, consisting of at least four broad and fairly strong bands superimposed on a strong continuum.

The position in energy of the Rydberg transitions converging to the ionic ground state and the successive ionic excited states are listed in Table 1.

4. AB initio calculations

The molecular orbital configuration of 1,1-$Br_2C_2F_2$ in the C_{2v} symmetry point group is described by:

$1s^2$(Br1) $1s^2$(Br2) $2s^2$(Br1) $2s^2$(Br2) $2p_{x,y,z}{}^6$(Br1) $2p_{x,y,z}{}^6$(Br2) $1s^2$(F3) $1s^2$(F4) $1s^2$(C1) $1s^2$(C2) $3s^2$(Br1) $3s^2$(Br2) $3p_{x,y,z}{}^6$(Br1) $3p_{x,y,z}{}^6$(Br2) $3d^{10}$(Br1) $3d^{10}$(Br2) $2s^2$(F3) $2s^2$(F4) $1a_1{}^2$ $1b_2{}^2$ $2a_1{}^2$ $3a_1{}^2$ $2b_2{}^2$ $1b_1{}^2$ $4a_1{}^2$ $1a_2{}^2$ $3b_2{}^2$ $5a_1{}^2$ $4b_2{}^2$ $2b_1{}^2$ $6a_1{}^2$ $2a_2{}^2$ $5b_2{}^2$ $3b_1{}^2$: $\tilde{X}{}^1A_1$

4.1. Computation

The Gaussian 09 program [10] has been used to perform the calculations presented in this work. The aug-cc-pVDZ basis set, containing polarization and diffuse functions, has been used for all the calculations [11].

The geometry optimization was performed at two calculation levels, i.e. M06-2X(DFT) [12] and TDDFT/M06-2X [13] in the C_{2v} symmetry point group. The vibrational wavenumbers were calculated at DFT/M06-2X and TDDFT/M06-2X levels.

4.2. Results of the Calculations

4.2.1. The neutral states

Only the optimized geometric parameters calculated in the C_{2v} symmetry point group for the neutral $\tilde{X}{}^1A_1$ state and a few allowed excited states are listed in Table S1 (see Supplementary material).

Only the geometry optimization of the $8{}^1B_1$ leads to a minimum in the C_{2v} symmetry point group. For the remaining neutral states the geometry could not be optimized owing to multiple surface crossings during the optimization process. In the C_S symmetry point group (i) the $12{}^1A_1$ state shows a minimum and (ii) the $3{}^1B_2$ and the lower lying $1{}^1B_1$ show the same geometry likely due to

Table 1
Rydberg series observed in the vacuum UV photoabsorption spectrum of 1,1-$Br_2C_2F_2$ converging to the successive ionization energies (IE) obtained in this work by quantum chemical calculations. Excitation energy (eV), wavenumber (cm^{-1}), effective quantum numbers (n^*), average quantum defects ($\bar{\delta}$) and assignments as proposed in this work. Conversion factor: 1 eV= 8065.545 eV [9].

This work		
eV	cm^{-1}	n^*
Rydb.Ser. to IE_{ad}=9.40 eV[a]		
$3b_1 \rightarrow ns$ ($\bar{\delta}$=2.98±0.04)		
6.18	49845	2.055
7.87	63476	2.982
$3b_1 \rightarrow np$ (δ=2.51)		
7.208	58136	2.491
$3b_1 \rightarrow nd$ (δ= 0.96)		
7.932	63976	3.044
Rydb.Ser. to IE_{ad}=10.94 eV[a]		
$5b_2 \rightarrow np$ ($\bar{\delta}$=2.55±0.03)		
8.611	69452	2.417
[9.820][c]	79204	3.485
10.254	82567	4.456
10.484	84559	5.462
Rydb.Ser. to IE_{vert}=11.76 eV[b]		
$2a_2 \rightarrow np$ ($\bar{\delta}$=2.55±0.06)		
9.422	75994	2.412
10.580	85333	3.395
11.096	89495	4.526
11.303	91165	5.456
$2a_2 \rightarrow nd$ ($\bar{\delta}$=1.01±0.05)		
10.186	82155	2.940
10.937	88213	4.041
Rydb.Ser. to IE_{ad}=11.91 eV[a]		
$6a_1 \rightarrow np$ ($\bar{\delta}$=2.48±0.05)		
[9.820][c]	79204	2.551
10.790	87027	3.485
$6a_1 \rightarrow nd$ (δ=0.99)		
10.373	83663	3.015
Rydb.Ser. to IE_{vert}=13.56 eV[b]		
$2b_1 \rightarrow np$ ($\bar{\delta}$=2.59±0.05)		
11.24	90657	2.42
12.42	100174	3.45
13.08	105497	5.32
$2b_1 \rightarrow nd$ ($\bar{\delta}$=1.14±0.01)		
11.80	95173	2.78
[12.64][c]	101948	3.84
13.28	107110	6.97
Rydb.Ser. to IE_{vert}=15.98 eV[b]		
[12.64][c]	95172	2.02 (5s)
13.78	111143	2.49 (5p)
14.40	116143	2.93 (4d)

[a] Adiabatic ionization energies obtained in this work by quantum chemical calculations.
[b] Vertical ionization energies obtained in this work by quantum chemical calculations.
[c] Different assignments could correspond to the excitation energy values in square brackets.

surface crossing. These findings are confirmed by the wavenumbers characterizing the vibrational normal modes of 1,1-$Br_2C_2F_2$. They are calculated for the neutral states in the C_{2v} symmetry point group and are schematically represented in FIG. S1 (see Supplementary material). Their values are listed in Table 2. Excepting the ground $\tilde{X}^1{}^1A_1$ and the excited 8^1B_1 states, all the other neutral states show one (TS transition states) or more (CP critical point states) imaginary values of the wavenumbers.

The 7^1A_1 transition state (TS) is characterized by an imaginary wavenumber of b_1 representation probably related to the abnormally high value for the ν_6 (a_2) wavenumber of 1081 cm-1.

The vertical and/or adiabatic excitation energies calculated in the C_{2v} point group for several neutral states are listed in Table 3a. A true adiabatic excitation energy has only been obtained for the 8^1B_1 state. The other values (in parentheses in Table 3a) are only indicative. The optimized geometry in the C_{2v} symmetry point group is not a minimum even at lower symmetry.

4.2.2. The ionized states

To the best of our knowledge, no photoionization data (HeI-PES, mass spectrometric electro- or photoionization) are available on 1,1-$Br_2C_2F_2$ in the literature. Therefore, quantum chemical calculations have been performed on the ionized states of this molecular system. The optimized geometry was calculated at the UM06-2X level for the $\tilde{X}^2B_1$, $\tilde{A}^2B_2$, $\tilde{B}^2A_2$ and $\tilde{C}^2A_1$ states and at the TDDFT level for the other states. The geometric parameters are listed in Table S2 (see Supplementary material). The $3b_1$ highest occupied molecular orbital (HOMO) corresponds to the π(C=C) bonding orbital. The following MO's, i.e. the $5b_2$, $2a_2$ and $6a_1$, are mainly centered on the vicinal Br atoms and are non-bonding. Table 4 displays the calculated adiabatic (IE_{ad}) and/or vertical (IE_{vert}) ionization energies characterizing the successive ionic states. These values will be adopted as the convergence limit for the Rydberg series classification (see Table 1).

Table 2
Calculated vibrational wavenumbers (cm^{-1}) for the neutral $\tilde{X}^1A_1$, 3^1B_2 and 4^1B_1 states at M02-6X level and the 7^1A_1, 8^1B_1, 10^1B_1 and 12^1A_1 states at the TDDFT/M02-6X level in the C_{2v} symmetry point group for 1,1-$Br_2C_2F_2$. The last column lists the data (in a' and a" representations) obtained for 12^1A" in the C_S symmetry point group. No scaling factor is applied to the calculated values. For the neutral ground state comparison is made with experimental data [2].

States	$\tilde{X}^1A_1$		3^1B_2	4^1B_1	7^1A_1	8^1B_1	10^1B_1	$12^1A_1(^1A")$	
Modes	Exp [2][a]	M06-2X	M06-2X		TDDFT				
								C_{2v}	C_S
a_1									
ν_1	1718	1819	1774	1591	1372	1584	1799	1942	**a'**
ν_2	1005	1043	989	1031	938	1037	979	971	2005
ν_3	598	599	548	573	558	623	562	562	1313
ν_4	324	335	235	355	313	353	204	262	1041
ν_5	203(R)	178	62	197	174	190	89	177	764
a_2									592
ν_6	151(R)	144	128	96	**1081**	95	107	**i54**	395
b_1									197
ν_7	572	572	566	349	106	716	585	609	100
ν_8	390	298	**i170**	**i1258**	**i2760**	357	180	**i94**	43
b_2									
ν_9	1307	1362	1299	1612	1386	1500	1358	1200	**a"**
ν_{10}	898	932	596	1250	995	1026	525	578	605
ν_{11}	399	412	100	398	334	404	140	101	224
ν_{12}	168(R)	152	**i821**	178	134	155	**i762**	**i613**	66

[a] All data are obtained by gas phase infrared spectroscopy: (R) refers to data obtained by Raman spectroscopy in the liquid phase.

Table 3
(a) Vertical (E_{vert}) and/or adiabatic (E_{ad}) excitation energies (eV) of neutral states of 1,1-$Br_2C_2F_2$ calculated at the TDDFT level in the C_{2v} symmetry point group. The calculations were carried out with the aug- cc-pVDZ basis set. (b) Structure and assignment for the 7^1A_1 (π^*) valence state. Conversion factor: 1 eV= 8 065.545 eV [9].

E_{vert}(eV)	E_{ad}(eV)	Description	
(a)			
6.08	(5.09)	$n_{Br} \rightarrow Rp_z$: 3^1B_2 (CP2)	
6.36	(6.06)	$\pi+n_{Br}+n_F \rightarrow$ Rs: 4^1B_1 (TS)	
6.5	?	$n_{Br} \rightarrow \sigma^*$(C-Br)	5^1A_1 (TS)
		$n_{Br} \rightarrow Rp_z$	
6.81	(6.21)	$\pi+n_{Br}+n_F \rightarrow \pi^*+n_{Br}+n_F$: 7^1A_1 (TS)	
7.38	7.09	$\pi+n_{Br}+n_F \rightarrow Rp_x$	8^1B_1
		$n_{Br} \rightarrow Rp_y$	
7.45	(6.07)	n_π(Br)$\rightarrow Rp_y$	10^1B_1 (TS)
		$\pi+n_{Br}+n_F \rightarrow Rp_z$	
7.59	(6.81)	$n_{Br} \rightarrow \sigma^*$(C-Br)	12^1A_1 (CP3)
		$n_{Br} \rightarrow Rp_y$	
(b)			
eV	cm^{-1}	Assignment	
6.595	53192	$7^1A_1(0,0)$	
6.760	54523	ν_1	$\omega_1{}^{av}$=0.163±0.003 eV
6.920	55814	$2\nu_1$	1315±20 cm^{-1}
7.085	57144	$3\nu_1$	

CP2 and CP3: second and third order critical point states. TS: transition states.

Table 4
Vertical (IE_{vert}) and adiabatic (IE_{ad}) ionization energies (eV) of 1,1-$Br_2C_2F_2$ determined at two calculation levels for the cationic states resulting from direct MO ionization.

Ion State	$\tilde{X}^2B_1$		$\tilde{A}^2B_2$		$\tilde{B}^2A_2$		$\tilde{C}^2A_1$	
Level	IE_{vert}	IE_{ad}	IE_{vert}	IE_{ad}	IE_{vert}	IE_{ad}	IE_{vert}	IE_{ad}
UM06-2X	9.71	9.40	11.51	10.94	11.86	11.57	12.61	11.91
TDDFT	9.70	9.40	11.05	-	11.76	-	11.82	-
	$\tilde{D}^2B_1$		$\tilde{E}^2B_2$		$\tilde{F}^2A_1$		$\tilde{G}^2B_2$	
TDDFT	13.56	13.23	14.45	14.08	15.67	15.43	15.98	15.48

It has to be noticed that above the $\tilde{E}^2B_1$ state doubly excited configurations occur. Furthermore, the $\tilde{E}^2B_2$ and the $\tilde{G}^2B_2$ states give rise to a surface crossing.

Table 5
Vibrational wavenumbers (cm^{-1}) calculated for the first seven ionized states of 1,1-$Br_2C_2F_2{}^+$ at the M06-2X ($\tilde{X}$-$\tilde{C}$) and TDDFT/M06-2X ($\tilde{D}$-$\tilde{F}$) levels in the C_{2v} symmetry point group. No scaling factor is applied to the calculated values.

State	$\tilde{X}^2B_1$	$\tilde{A}^2B_2$	$\tilde{B}^2A_2$	$\tilde{C}^2A_1$	$\tilde{D}^2B_2$	$\tilde{E}^2B_1$	$\tilde{F}^2A_1$
TDDFT/M06-2X							
a_1							
$\nu_1{}^+$	1622	1833	1798	1742	1735	1755	1553
$\nu_2{}^+$	1070	1104	1083	1048	1063	1066	984
$\nu_3{}^+$	640	619	610	590	602	571	575
$\nu_4{}^+$	354	339	335	317	288	258	275
$\nu_5{}^+$	191	159	171	177	148	136	137
a_2							
$\nu_6{}^+$	88	142	140	138	97	157	134
b_1							
$\nu_7{}^+$	652	639	659	640	620	648	609
$\nu_8{}^+$	318	209	273	244	231	152	231
b_2							
$\nu_9{}^+$	1529	1445	1443	1430	1489	1424	1551
$\nu_{10}{}^+$	1027	842	735	899	1018	381	1229
$\nu_{11}{}^+$	409	393	382	400	395	263	428
$\nu_{12}{}^+$	160	113	141	160	135	106	168

The wavenumbers characterizing the twelve vibrational coordinates of 1,1-$Br_2C_2F_2{}^+$ have been calculated for the $\tilde{X}^2B_1$ to the $\tilde{H}^2B_2$ ionic states. Only the results concerning $\tilde{X}^2B_1$ to the $\tilde{F}^2A_1$ are listed in Table 5. No scaling factor has been applied.

5. Discussion of the experimental data

For the Rydberg series analysis the simplest model neglects the Rydberg-Rydberg interactions. The energy position of the members of a series (E_{Ryd}) being fitted by the Rydberg formula:

$$E_{Ryd} = IE - R/(n-\delta)^2 = IE - R/(n*)^2 \quad (1)$$

R is the Rydberg constant R=13.6057 eV [9], δ is the quantum defect, n* is the effective quantum number and IE is the convergence limit of the considered Rydberg series. The successive ionization energies IE to be used have been defined in Section 4.2.2 and are listed in Table 3. The adiabatic ionization energy (IE_{ad}) has been adopted for excitations where the (0,0) vibrational transition has been identified. Otherwise, the vertical ioniza-

tion energy (IE_{vert}) has been chosen as the convergence limit. The $R/(n^*)^2$ is the term value T of the considered Rydberg series. Trend values of T (δ or n^* implicitly) characterizing ns-, np- and nd-type Rydberg series are observed and have been widely discussed [14].

5.1. The Transitions between 5.0 eV and 7.1 eV (see Figs. 1 and 2a)

The characteristic broad band observed at low energy in the vacuum UV PAS of the ethylene compounds has its maximum at 6.920 eV (55814 cm^{-1}) in 1,1- $Br_2C_2F_2$ and is shown in Fig. 1. In Fig. 2a this photon energy range is shown on an expanded energy scale. The red curve in the upper part of the figure represents the continuum subtracted from the original signal. The resulting Δ-plot displayed in the lower part of Fig. 2a clearly shows three different features: (i) up from 5.2 eV, a broad slowly- rising continuous absorption, (ii) around 6.0 eV a step-like continuous signal and (iii) up from 6.5 eV four broad but well-resolved peaks spreading up to 7.1 eV. Their energy positions are listed in Table 3b.

For the assignment of the features observed in this energy region quantum chemical calculations have been performed. Several neutral states have been calculated at the C_{2v} symmetry point group between 5.1 eV and 7.1 eV. Their optimized geometry and vibrational wavenumbers were obtained. Only those allowed to be reached from the $\tilde{X}^1A_1$ neutral ground state with significant oscillator strength are listed in Table S1 and Table 2. The corresponding excitation energies (adiabatic and/or vertical) are displayed in Table 3a.

First, the lowest energy part extending between 5.2 eV and 6.0 eV is likely consisting of two very weak broad bands. By quantum chemical calculations the lowest transition energy to be observed corresponds to the $\tilde{X}^1A_1 \rightarrow 3^1B_2$ valence transition at $E_{exc}{}^{ad}$=5.09 eV and $E_{exc}{}^{vert}$=6.08 eV. As shown in Table 2 and Table S1 the 3^1B_2 is a second order critical point state in the C_{2v} symmetry point group. It shows a very large increase of both the C-Br internuclear distance (2.1462 Å) and the C=C-Br angle (134.04°). It should be assigned to the $n_{Br} \rightarrow Rp_z$ valence excitation. Transitions to the lower lying 1^1B_1 ($E_{exc}{}^{vert}$=4.90 eV) and 2^1A_1 ($E_{exc}{}^{vert}$=5.25 eV) are too weak and energetically too low or not allowed.

Second, at 6.0 eV the absorbance significantly increases and levels off up to 6.5 eV. No significant structure is observed. In the Δ-plot displayed in Fig. 2a a maximum is observed at 6.18 eV (49845 cm^{-1}). By the calculations performed in the present work a $\pi+n_{Br}+n_F \rightarrow 4^1B_1(5s)$ Rydberg transition is obtained at $E_{exc}{}^{vert}$=6.36 eV and $E_{exc}{}^{ad}$=6.06 eV. The final 4^1B_1 state, of Rydberg character, should be a transition state as shown in Table 2. Essentially the internuclear distances are considerably modified (see Table S1): the C-F and C-Br are reduced whereas the C=C is markedly extended. Using the predicted $IE_{ad}(\tilde{X}^2B_1)$=9.40 eV (75816 cm^{-1}) for the first ionization energy limit of 1,1-$Br_2C_2F_2$ and the measured E_{exc}=6.18 eV a quantum defect δ=2.945 is obtained and is compatible with a 5s-Rydberg state.

Finally, a progression of four regularly spaced and comparatively narrow peaks is starting at 6.595 eV (53192 cm^{-1}). The maximum intensity is observed at 6.920 eV (55814 cm^{-1}). The energy positions are listed in Table 3b and the average spacing is 1315±20 cm^{-1} (0.163±0.003 eV). By quantum chemical calculation the 7^1A_1 state is predicted at $E_{exc}{}^{ad}$=6.21 eV and $E_{exc}{}^{vert}$=6.81 eV. This is a valence state described by ($\pi^*+n_{Br}+n_F$) character. It shows a very strong increase of the C=C internuclear distance whereas the C-Br distance is reduced. Vibrational wavenumbers associated with this valence state have been calculated and are listed in Table 2. The strong C=C distance alteration would mainly induce the C=C stretching vibration calculated at 1372 cm^{-1}. This predicted value has to be compared with the experimental $\omega_1{}^{av}$=1315±20 cm^{-1}. The width of the four peaks is likely to be linked with the lifetime of the vibrational states of 7^1A_1 which is a transition state in the C_{2v} symmetry point group. The high imaginary wavenumber of i2760 cm^{-1} is likely induced by the unusually high wavenumber of 1081 cm^{-1} calculated for the $\nu_6(a_2)$ vibrational mode. In the neutral ground state the corresponding wavenumber is 151 cm^{-1} [2].

5.2. Rydberg Transitions between 7.1 eV and 11.5 eV (see Figs. 1 and 2b-d)

5.2.1. Rydberg series converging to $\tilde{X}^2B_1$ at IE_{ad}= 9.40 eV

As mentioned in Table 1 only weak and short Rydberg series converging to IE_{ad}=9.40 eV are observed: ns (n=5 and 6) with $\bar{\delta}$=2.98±0.04, the 5p with δ=2.51 and the 4d with δ= 0.96.

The $3b_1(\pi) \rightarrow 5s$ transition observed at 6.18 eV has already been described in Section 5.1 and has been identified as the 4^1B_1 state. The second member of this series is likely buried in the continuum underlying the weak structured part of the spectrum between 7.8 eV and 8.5 eV. Fig. 2b clearly shows a steep increase of the absorption at 7.85 eV. Taking the maximum observed at 7.87 eV in the corresponding Δ-plot δ= 3.018 is obtained and is compatible with an 6s-type Rydberg state.

As shown in Fig. 2a and 2b above the vibrational progression pertaining to the 7^1A_1 (or π^*) state a series of narrow structures are observed between 7.2 eV and 7.8 eV. The first transition is measured at 7.208 eV. Assuming this energy being the $E_{exc}{}^{ad}$ a quantum defect value δ= 2.509 is obtained and is clearly indicative of a p-type Rydberg state.

The quantum chemical calculations performed in the present work provide a 8^1B_1 neutral state involved in the $(\pi+n_{Br}+n_F) \rightarrow Rp_x(5p)$ Rydberg transition with $E_{exc}{}^{ad}$=7.09 eV and $E_{exc}{}^{vert}$=7.38 eV. This neutral state is the only state showing a minimum in the geometry optimization in the C_{2v} symmetry point group. Mainly the C-Br and C-F internuclear distances are shortened whereas the C=C distance is considerably lengthened. The valence angles slightly decrease. From this description the excited vibrational modes to be observed in the absorption are expected to involve these modifications.

The vibrational analysis proposed for this transition is presented in Table 6. The vibrational transitions to the 8^1B_1 state could be accounted for by the combination of four vibrational normal modes: ν_1(C=C stretching), ν_2(C-F stretching), ν_3(C-F bending) and ν_4(C-Br stretching/C-F bending). The averaged vibrational wavenumbers provided by the experiment are ω_2=940±20 cm^{-1} (116±2 meV), ω_3=580±30 cm^{-1} (72±4 meV) and ω_4=330±20 cm^{-1} (41±2 meV). For ω_1 the most appropriate value is obtained by the extrapolation of the E_v–versus-v or ΔG_v-versus-v diagram shown in Fig. 3. Both provide ω_1=1510±20 cm^{-1} (187±2 meV). A small anharmonicity ω_1x_1 is also obtained.

These experimental values have to be compared with those predicted for the neutral Rydberg state 8^1B_1, i.e. ω_1=1584 cm^{-1}, are ω_2=1037 cm^{-1}, ω_3=623 cm^{-1} and ω_4=353 cm^{-1} (Table 2). Furthermore, the experimental excitation energies $E_{exc}{}^{ad}$=7.208 eV and $E_{exc}{}^{vert}$= 7.394 eV are in satisfactory agreement with the predicted values. In the frame of our hypotheses, a comparison could be allowed with the vibrational wavenumbers calculated for the ionized $\tilde{X}^2B_1$ ground state, i.e. $\omega_1{}^+$=1622 cm^{-1}, $\omega_2{}^+$=1070 cm^{-1}, $\omega_3{}^+$=640 cm^{-1} and $\omega_4{}^+$=354 cm^{-1} (Table 5). The correctness of the assumption is also strengthened by the close similarity of the geometrical parameters of the neutral 8^1B_1 and the ionized $\tilde{X}^2B_1$ states shown in Tables S1 and S2. From these assumptions the HeI-PES band of the 1,1-$Br_2C_2F_2{}^+$ ($\tilde{X}^2B_1$) is expected to have about the same Franck-Condon profile as the 8^1B_1 Rydberg state.

As shown in Fig. 2b and 2c a long progression is starting at 7.932 eV. Using this excitation energy and IE_{ad}=9.40 eV, an effective quantum number n^*=3.04 and a quantum defect δ= 0.96 are obtained. Both values pinpoint a 4d-Rydberg state. This progression likely extends up to 9.184 eV. Several weak features are superim-

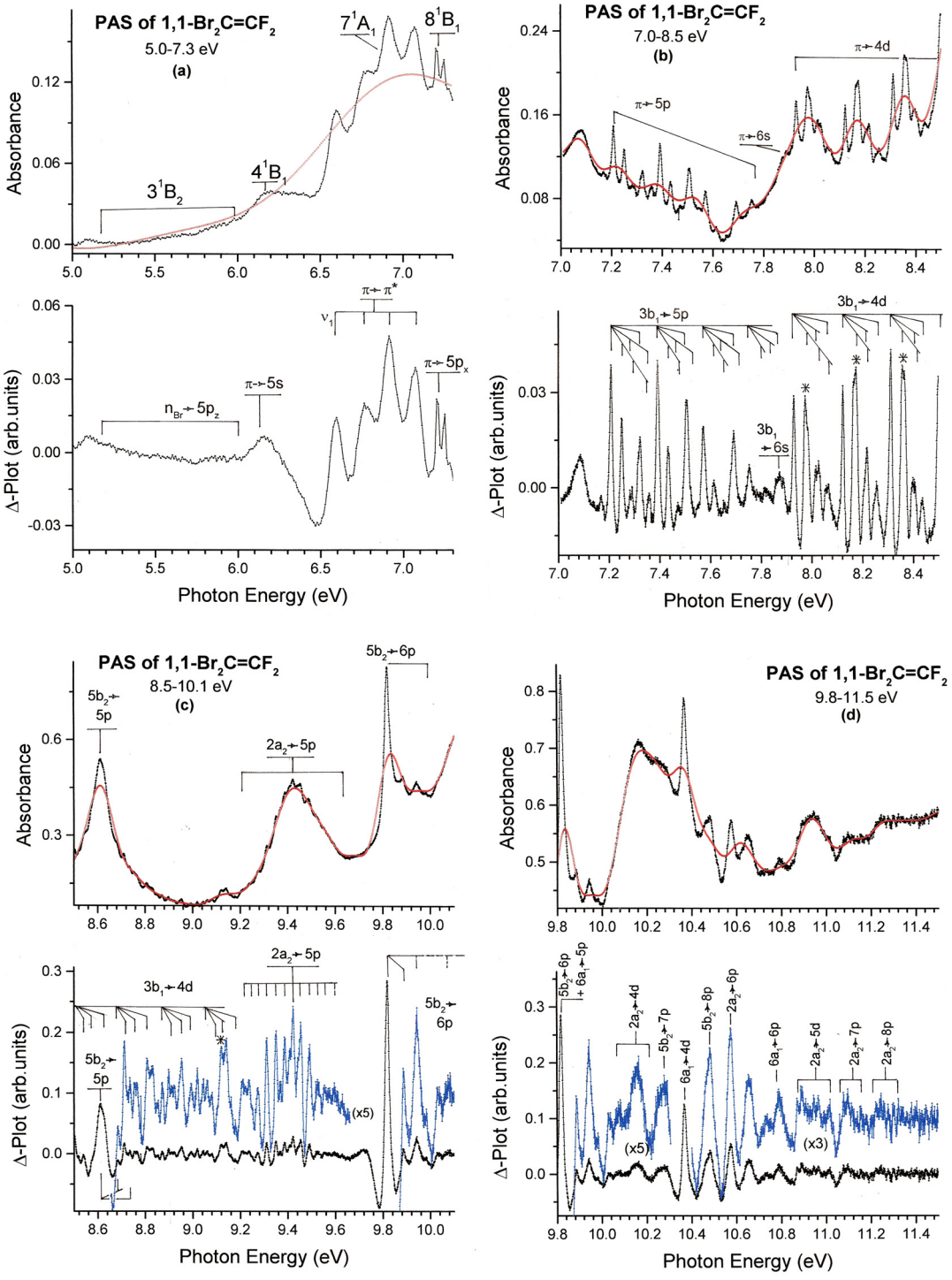

Fig. 2. VUV photoabsorption spectrum of 1,1-$Br_2C_2F_2$ on an expanded photon energy scale between 5.0 eV and 14.7 eV. The upper and lower panels show the absorbance and the corresponding Δ-plot respectively for (a) 5.0–7.3 eV, (b) 7.0–8.5 eV, (c) 8.5–10.1 eV, (d) 9.8–11.5 eV and (e) 11.0–14.7 eV. The red curve in the upper panels corresponds to the continuum used for subtraction leading to the Δ-plot. For each Rydberg transition the progression(s) is (are) drawn by short vertical bars. Square brackets define the energy range for the indicated Rydberg transitions. Shaded areas correspond to the convergence limits (adiabatic or vertical ionization energies) calculated in the present work.

posed on a strong narrow absorption band at 8.611 eV. These are best highlighted in the Δ-plot diagram shown in the lower panel of Fig. 2c. The energy position is listed in Table 6.

From the vibrational analysis of the 4d-Rydberg state five vibrational wavenumbers are derived accounting for the observations. Their averaged values are ω_2=1010±40 cm^{-1} (125±5 meV), ω_3= 655±30 cm^{-1} (81±4 meV), ω_4= 380±40 cm^{-1} (47±5 meV) and ω_5=185±30 cm^{-1} (23±4 meV). The ω_1 value has been deduced from the extrapolation of the E_v–versus-v or ΔG_v-versus-v diagram shown in Fig. 4. In both cases ω_1^{ex}=1540±20 cm^{-1} (191±3 meV) is obtained. From these diagrams no significant value of the anharmonicity $\omega_1 x_1$ could be inferred.

Compared to the 5p-Rydberg state, several differences of the 4d-Rydberg state have to be pointed out. Mainly, the Franck-

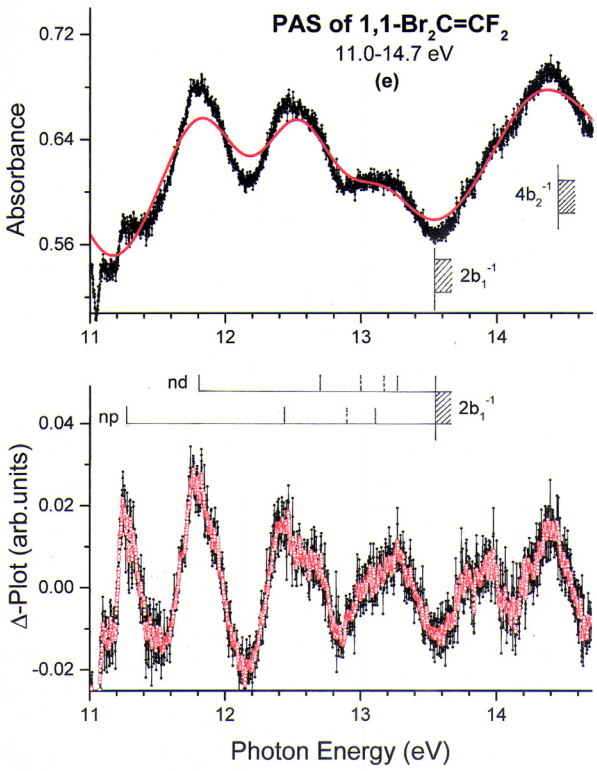

Fig. 2. Continued

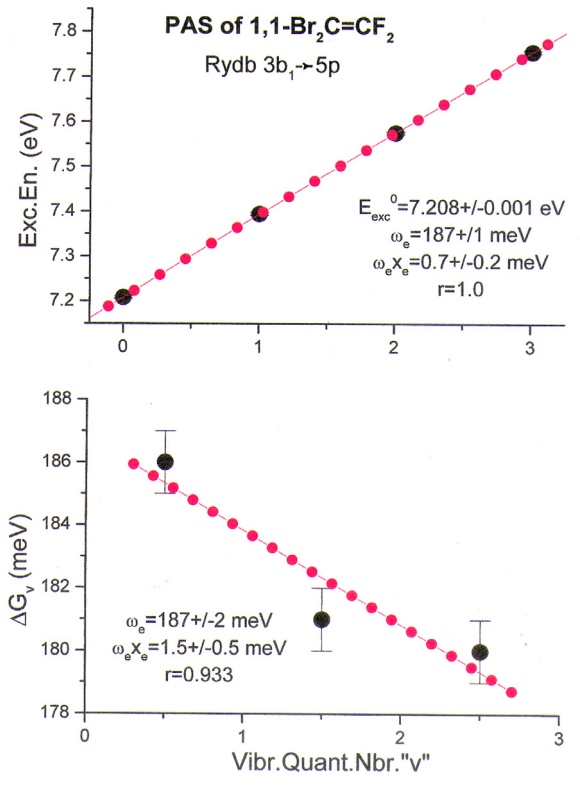

Fig. 3. Excitation energy (Exc.En.) (upper panel) and ΔG_v (lower panel)-vs- vibrational quantum number v-plots for the $3b_1^{-1} \rightarrow 5p$ Rydberg transition for 1,1-$Br_2C_2F_2$. Experimental values (black points), least square fittings (red circles) and fitting parameters are inserted.

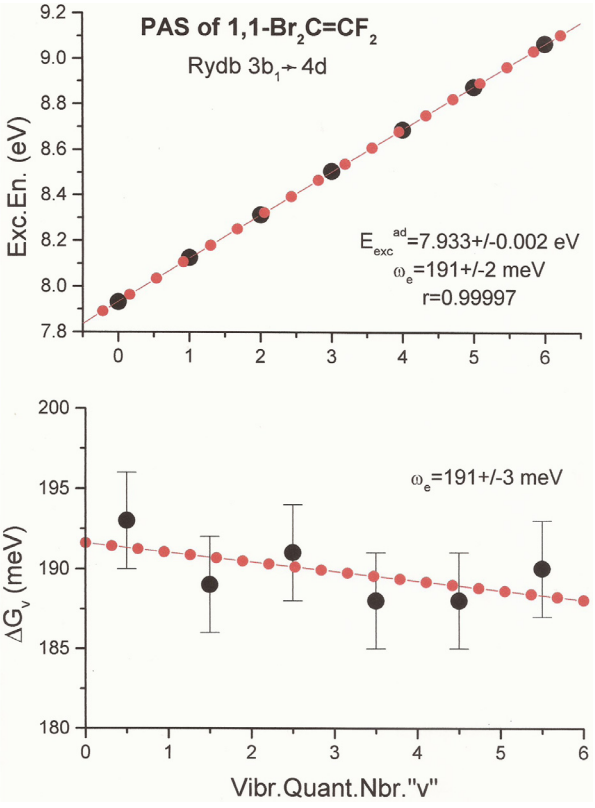

Fig. 4. Excitation energy (Exc.En.) (upper panel) and ΔG_v (lower panel)-vs- vibrational quantum number v-plots for the $3b_1^{-1} \rightarrow 4d$ Rydberg transition for 1,1-$Br_2C_2F_2$. Experimental values (black points), least square fittings (red circles) and fitting parameters are inserted.

Table 6
Energy position (eV), wavenumber (cm^{-1}) and assignments proposed for the vibrational structure of Rydberg states observed in the vacuum UV photoabsorption spectrum of 1,1-$Br_2C_2F_2$ between 7.2 eV and 9.2 eV and converging to the $\tilde{X}^2B_1$ ionic ground state. Conversion factor 1 eV= 8 065.545 cm^{-1} [9].

This work			
Energy[b] (eV)	Wavenbr. (cm^{-1})	Assignment	
$3b_1 \rightarrow 5p$ (8^1B_1)			
7.208	58136	**(0,0)**	ω_1^{ex}=187±2 meV[a]
7.250	58483	ν_4	1510±20 cm^{-1}
7.280(5)	58717	ν_3	$\omega_1 x_1$=1.5±0.5 meV
7.287(4)	58774	$2\nu_4$	12±4 cm^{-1}
7.317	59016	n.a.	ω_2=116±2 meV
7.322	59056	ν_2	940±20 cm^{-1}
7.336	59169	$3\nu_4$	ω_3=72±4 meV
7.353	59306	$2\nu_3$	580±30 cm^{-1}
7.364(5)	59395	$\nu_2+\nu_4$	ω_4=41±2 meV
7.394	59637	$\boldsymbol{\nu_1}$	330±20 cm^{-1}
7.434	59959	$\nu_1+\nu_4$	
7.466	60217	$\nu_1+\nu_3$	
7.475(5)	60290	n.a.	
7.478	60314	$\nu_1+2\nu_4$	
7.507	60548	$\nu_1+\nu_2$	
7.546	60862	$\nu_1+\nu_2+\nu_4$	
7.572	61072	$\boldsymbol{2\nu_1}$	
7.613	61403	$2\nu_1+\nu_4$	
7.637(7)	61597	$2\nu_1+\nu_3$	
7.654	61734	$2\nu_1+2\nu_4$	
7.693(4)	62048	$2\nu_1+\nu_2$	
7.755	62548	$\boldsymbol{3\nu_1}$	
7.794	62863	$3\nu_1+\nu_4$	
7.825	63113	$3\nu_1+\nu_3$	
7.859(5)	63387	$3\nu_1+\nu_3+\nu_4$	
7.873	63500	$3\nu_1+\nu_2$	
7.889	63629	$3\nu_1+2\nu_3$	
$3b_1 \rightarrow 4d$			
7.932	63960	**(0,0)**	ω_1^{ex}=191±3 meV
7.952	64137	ν_5	1540±24 cm^{-1}
7.975	64323	$2\nu_5$	ω_2=125±5 meV
7.986	64411	ν_4	1010±40 cm^{-1}
8.014	64637	ν_3	ω_3=81±4 meV
8.024(5)	64718	$2\nu_4$	655±30 cm^{-1}
8.031	64774	n.a.	ω_4=47±5 meV
8.057	64984	ν_2	380±40 cm^{-1}
8.067	65065	$3\nu_4$	ω_5=23±4 meV
8.092	65266	$2\nu_3$	185±30 cm^{-1}
8.123	65516	$\boldsymbol{\nu_1}$	
8.147	65710	$\nu_1+\nu_5$	
8.166	67896	$\nu_1+2\nu_5$	
8.177	65952	$\nu_1+\nu_4$	
8.204	66170	$\nu_1+\nu_3$	
8.215	66258	$\nu_1+2\nu_4$	
8.245	66500	$\nu_1+3\nu_4$	
8.257(7)	66597	$\nu_1+\nu_2$	
8.271	66710	$\nu_1+4\nu_4$	
8.292	66879	$\nu_1+2\nu_3$	
8.313	67049	$\boldsymbol{2\nu_1}$	
8.337	67242	$2\nu_1+\nu_5$	
8.359	67420	$2\nu_1+\nu_4$	
8.366	67476	$2\nu_1+2\nu_5$	
8.400	67750	$2\nu_1+\nu_3$	
8.409	67823	$2\nu_1+2\nu_4$	
8.436	68041	$2\nu_1+\nu_2$	
8.466	68283	$2\nu_1+3\nu_4$	
8.501	68565	$\boldsymbol{3\nu_1}$	
8.521	68727	$3\nu_1+\nu_5$	
8.543(4)	68904	$3\nu_1+\nu_4$	
8.575(6)	69162	$3\nu_1+\nu_3$	
8.611	69452	$\underline{5b_2 \rightarrow 5p}$	
8.625	69565	$3\nu_1+\nu_2$	
8.635	69646	$3\nu_1+3\nu_4$	
[8.686(6)][c]	70057	$\boldsymbol{4\nu_1}$	
[8.715][c]	70291	$4\nu_1+\nu_5$	
8.738	70477	$4\nu_1+2\nu_5$	
8.768(5)	70719	$4\nu_1+\nu_3$	
8.782	70832	$4\nu_1+2\nu_4$	

(continued on next column)

Table 6
(continued)w

This work		
Energy[b] (eV)	Wavenbr. (cm^{-1})	Assignment
8.808	71041	$4\nu_1+\nu_2$
8.875(4)	71582	$\boldsymbol{5\nu_1}$
8.902	71799	$5\nu_1+\nu_5$
8.916(4)	71912	n.a.
8.925	71985	$5\nu_1+\nu_4$
8.956(4)	72235	$5\nu_1+\nu_3$
8.993	72533	$5\nu_1+\nu_2$
9.065	73114	$\boldsymbol{6\nu_1}$
9.085	73275	$6\nu_1+\nu_5$
9.102(4)	73413	$6\nu_1+2\nu_5$
9.122	73574	$6\nu_1+\nu_4$
9.144	73751	$6\nu_1+\nu_3$
9.163(4)	73905	$6\nu_1+2\nu_4$
9.184	74074	$6\nu_1+\nu_2$

[a] ω_1^{ex} stands for the corresponding ω_e value obtained by extrapolation. Other ω_i are averaged values.
[b] When the dispersion on the energy position averaged over 7 measurements is larger than 3 meV its value is mentioned in parentheses.
[c] To the excitation energy values in square brackets could correspond different assignments.

Condon band profile is quite different: (i) the main vibrational progression is longer, extending likely up to $6\nu_1$, (ii) the E_{exc}^{vert} is shifted to $2\nu_1$, (iii) a fifth vibrational wavenumber ω_5=185±30 cm^{-1} is detected owing to the presence of two close-lying, slightly resolved components (marked by an asterisk in Fig. 2b and 2c). Therefore, unusual vibrational intensity distributions are observed within the vibrational progression of the 4d-Rydberg state.

The last observation is particularly related to the intensity of the ν_4 and ν_5 vibrations with ω_4=380±40 cm^{-1} and ω_5=185±30 cm^{-1} respectively where the fundamental ν_4 has about twice the wavenumber of ν_5, i.e. $2\omega_5 \approx \omega_4$. It is obviously the case when the error limits are taken into account. Both vibrational modes are of the same a_1 species. The relative intensity of the corresponding transitions is considerably enhanced.

The other observations mentioned above would likely be indicative for the vibronic perturbation of the 4d-Rydberg state by the underlying and nearly degenerate 6s-state [15]. This latter state is possibly a transition state similar to the 5s-member of this Rydberg series.

5.2.2. Rydberg series converging to $IE_{ad}(\tilde{A}^2B_2)$=10.94 eV, $IE_{vert}(\tilde{B}^2A_2)$=11.76 eV and $IE_{ad}(\tilde{C}^2A_1)$=11.91 eV

The Rydberg transitions involving the $5b_2$-, $2a_2$- and the $6a_1$-MO are related to the lone-pair orbitals mainly centered on the Br atoms as illustrated in Fig S2 (see Supplementary Material). The corresponding adiabatic and vertical ionization energies are obtained by quantum chemical calculations. The large intensity of the absorption bands involving these three transitions is used as a guide for the assignment. Table 1 displays a classification of bands assigned to Rydberg series converging to these three ionic states.

For the $5b_2 \rightarrow R(n\ell)$ Rydberg transitions starting at 8.611±0.002 eV only np-type Rydberg series (n=5-8) could be highlighted. The corresponding bands are the strongest of the PAS and are very sharp showing narrow vibrational progressions, pointing out the non-bonding character of the $5b_2$ MO. The average quantum defect $\bar{\delta}$=2.55±0.03 is obtained using $IE_{ad}(\tilde{A}^2B_2)$=10.94 eV provided by the quantum chemical calculations performed in the present work. No or very few and very weak vibrational structures are associated with these transitions. The 5p-member is strongly overlapped by the $3b_1 \rightarrow 4d$ vibrational progression. The $5b_2 \rightarrow 6p$ transition at 9.820±0.002 eV is well isolated and clearly shows two very weak and sharp features at 9.887±0.002 eV and at 9.946±0.004 eV suc-

Table 7
Energy position (eV), wavenumber (cm^{-1}) and assignments proposed in the present work for the vibrational structure observed in the vacuum UV photoabsorption spectrum of 1,1-$Br_2C_2F_2$ between 9.2 eV and 9.6 eV and converging to the $\tilde{B}^2A_2$ ionized state. Conversion factor 1 eV= 8065.545 eV [9].

Energy[a] (eV)	Wavenbr. (cm^{-1})	Assignment	
$2a_2 \rightarrow 5p$			
9.208	74268	**(0,0)**	ω_A=35±3 meV
9.225	74405	ν_B	280±20 cm^{-1}
9.241	74534	$\boldsymbol{\nu_A}$	ω_B=16±5 meV
9.253	74630	$\nu_A+\nu_B$	130±40 cm^{-1}
9.276	74816	$\mathbf{2\nu_A}$	
9.296(4)	74977	$2\nu_A+\nu_B$	The inferred
9.314(4)	75122	$\mathbf{3\nu_A}$	**IE_{ad}= 11.47 eV**
9.340	75332	$3\nu_A+\nu_B$	for the $\tilde{B}^2A_2$
9.352	75429	$\mathbf{4\nu_A}$	
9.370	75574	$4\nu_A+\nu_B$	
9.388	75719	$\mathbf{5\nu_A}$	
9.410	75897	$5\nu_A+\nu_B$	
9.422(Max)	75994	$\mathbf{6\nu_A}$	
9.443	76163	$6\nu_A+\nu_B$	
9.455	76260	$\mathbf{7\nu_A}$	
9.492	76558	$\mathbf{8\nu_A}$	
9.518	76768	$8\nu_A+\nu_B$	
9.527(5)	76840	$\mathbf{9\nu_A}$	
9.558	77090	$\mathbf{10\nu_A}$	
9.573	77211	$10\nu_A+\nu_B$	
9.595(6)	77389	$\mathbf{11\nu_A}$	

[a] When the dispersion on the energy position averaged over 7 measurements is larger than 3 meV its value is mentioned in parentheses.

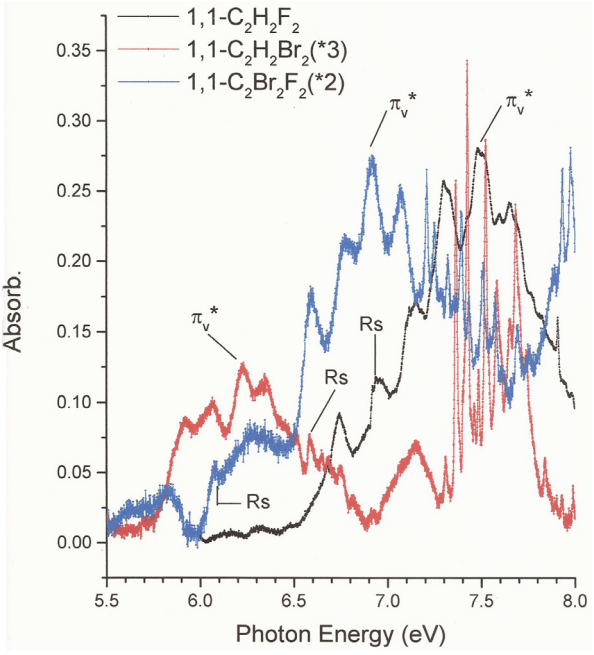

Fig. 5. VUV photoabsorption spectra of 1,1-$F_2C_2H_2$, 1,1-$Br_2C_2H_2$ and 1,1-$Br_2C_2F_2$ on an expanded photon energy scale between 5.5 eV and 8.0 eV. The vertical (index v) and the adiabatic excitation energies of the Rydberg (Rs) transitions are indicated for each molecule.

cessively. To the energy differences of 67±4 meV and 126±6 meV correspond ω_A=540±24 cm^{-1} and ω_B=1016±60 cm^{-1} respectively. These wavenumbers could correspond to ν_3 and ν_2 when compared to the wavenumbers predicted for the $\tilde{A}^2B_2$ ionic state where ω_3^+=619 cm^{-1} and ω_2^+=1104 cm^{-1}.

For the $2a_2 \rightarrow R(n\ell)$ Rydberg transitions likely $2a_2 \rightarrow np$ (n=5-8) and $2a_2 \rightarrow nd$ (n=4, 5) series have been identified. The first member of the former series shows a maximum intensity at 9.422±0.002 eV corresponding to the maximum of the strong broad band. The latter series starts at 10.186 eV. Using the convergence limit $IE_{vert}(\tilde{B}^2A_2)$=11.76 eV, as predicted in the calculations of the present work, average quantum defects $\bar{\delta}_{np}$=2.55±0.06 and $\bar{\delta}_{nd}$= 1.01±0.05 are obtained. Only the 5p-member is fairly completely isolated. The application of the subtraction procedure to this peak yields the result shown in the lower panel of Fig. 2c. It clearly shows a long vibrational progression extending between 9.208 eV and 9.595 eV. The energy position of the successive features is listed in Table 7. Its analysis provides two wavenumbers, i.e. ω_A= 280±20 cm^{-1} and ω_B=130±40 cm^{-1}. Referring to the wavenumbers predicted for the $\tilde{B}^2A_2$ ionic state these figures should be compared to ω_4^+=335 cm^{-1} and ω_5^+=171 cm^{-1}. Assuming E_{exc}^{ad}=9.208 eV and taking $\bar{\delta}_{np}$=2.55 a term value T=2.267 eV and $IE_{ad}(\tilde{B}^2A_2)$=11.47 eV are obtained. This figure is in good agreement with 11.57 eV predicted by the calculations. Tentatively, the higher members of both the np- and nd-series are shown in Fig. 2d by brackets spanning the energy region of vibrational structures.

Taking IE_{ad}=11.91 eV calculated for the ionization involving the $6a_1$ MO and the excitation energy at 9.820 eV n*=2.55 and δ=2.48 are obtained. The strong narrow band at 9.820 eV could involve the $6a_1 \rightarrow 5p$ Rydberg transition. However, as discussed earlier in this section, this excitation energy was assigned to $5b_2 \rightarrow 6p$ Rydberg transition. Very likely both transitions take place and share the intensity observed at 9.820 eV. The $6a_1 \rightarrow 4d$ Rydberg transition is assigned to the sharp feature observed at 10.373 eV.

5.3. Rydberg Transitions between 11.0 eV and 15.0 eV (see Figs. 1 and 2e)

This part of the vacuum UV PAS is made of broad bands of medium intensity superimposed on a strong continuum as shown in Fig. 1. To highlight the presence of structure in this part of the spectrum the subtraction method has been applied. The result is shown in the lower panel of Fig. 2e. Because of the unfavorable signal/noise ratio a slight smoothing by Fourier transform (FFT) has been applied (red circles). The positions in energy of the maximum for the successive features are listed in Table 1. This will implicitly lead us to use the calculated IE_{vert} convergence limits.

The sharpest band in this energy range lies at 11.24 eV. Presumably this feature is the first member of an np-Rydberg series converging to the $2b_1^{-1}$ ionization limit calculated at IE_{vert}= 13.56 eV. Two other members, i.e. the 6p and 8p Rydberg states, could tentatively be assigned to the maxima observed at 12.42 eV and 13.08 eV respectively. An average quantum defect $\bar{\delta}$=2.59±0.05 is derived. Above 11.6 eV the observed broadness of the bands could at least partially be attributed to their splitting in at least two contributions. Below IE_{vert}=13.56 eV a second Rydberg series could be present, likely corresponding to an nd-series, characterized by $\bar{\delta}$=1.14±0.01.

Above 13.6 eV three peaks are observed at 13.78/13.95 eV and 14.4 eV. The corresponding transitions would involve Rydberg states converging to ionized states lying above 13.56 eV. Three ionization continua are predicted successively at $IE_{vert}(4b_2^{-1})$=14.45 eV, $IE_{vert}(5a_1^{-1})$=15.67 eV and $IE_{vert}(3b_2^{-1})$=15.98 eV. The transition at 13.08 eV, tentatively assigned to $2b_1^{-1} \rightarrow 8p$ Rydberg transition, could possibly also be assigned to $4b_2^{-1} \rightarrow 5d$ Rydberg transition with n*=3.14. None of the observed features seem to correspond to $5a_1^{-1} \rightarrow R(n\ell)$ Rydberg transitions. These are likely hidden in the unresolved components of the bands shown in Fig. 2e.

However, it has to be mentioned that the two highest energy bands, i.e. at 13.78 eV and 14.40 eV, provide term values of 2.20

eV and 1.58 eV with respect to $IE_{vert}(3b_2^{-1})$=15.98 eV. These could correspond to $3b_2^{-1}\rightarrow 5p$ (n^*=2.49) and 4d (n^*=2.93) Rydberg transitions. The band at 12.64 eV, assigned earlier to $2b_1^{-1}\rightarrow 5d$, could also correspond to a $3b_2^{-1}\rightarrow 5s$ (n^*=2.02) transition with a term value of 3.34 eV.

6. Conclusions

For the first time the vacuum UV PAS of 1,1-$Br_2C_2F_2$ has been measured using synchrotron radiation. The data have been examined in the light of the results obtained by quantum chemical calculations applied to the neutral and ionized states of this molecule.

At low energy, beside the $\pi\rightarrow\pi^*$ valence transition, also Rydberg transitions have been identified converging to the lowest ionization energy predicted at $IE_{ad}(3b_1^{-1})$=9.40 eV by quantum chemical calculations. Only the 5p and 4d members of the series are observed showing vibrational progressions. The latter state is found to be perturbed likely by the nearly resonant 6s-Rydberg state. An unusual vibrational intensity distribution in the 4d-state has been strengthened. An attempt to assign Rydberg series converging to higher IE has been presented.

At medium energy, several Rydberg series are detected in the PAS converging to higher ionization limits, i.e. the $\tilde{A}^2B_2$, $\tilde{B}^2A_2$ and $\tilde{C}^2A_1$ ionized states calculated at 10.94 eV, 11.76 eV and 11.91 eV respectively. Short vibrational progressions are observed.

At the high energy side of the PAS, superimposed on a strong continuum, four strong bands are observed. These are likely consisting of several Rydberg series converging to higher ionization limits. An interpretation and assignments of these features have been attempted.

At the present state of our investigation of the halogenated derivatives of ethylene a comparison could be made with the low-energy side of the vacuum UV PAS of 1,1-$C_2H_2F_2$ [15] and 1,1-$C_2H_2Br_2$ [4]. In the range of 5.0 eV to 8.0 eV the most important features are the $\pi(nb_1)\rightarrow\pi^*$ valence- and the lowest Rydberg $\pi(nb_1)\rightarrow$Rs Rydberg transitions. As shown in Fig. 5, the $E_{exc}{}^{vert}(\pi_v{}^*)$ for the valence transition is considerably shifted to lower energy 1,1-$H_2C_2F_2$>1,1-$Br_2C_2F_2$>1,1-$Br_2C_2H_2$ at 7.482 eV [16], 6.920 eV and 6.231 eV [4] respectively. With respect to 1,1-$Br_2C_2H_2$ [4] the π^* state is strongly stabilized, i.e. +0.689 eV, by the 2,2-substitution of H_2 by F_2. Contrarily, the lowest Rs Rydberg state is continuously destabilized on substitution 1,1-$H_2C_2F_2$>1,1-$Br_2C_2H_2$>1,1-$Br_2C_2F_2$ at 6.957 eV [16], 6.583 eV [4] and 6.18 eV respectively. This sequence logically follows the trend of the ionization energy IE_{vert} of the respective $\tilde{X}^2B_1$ ground state, i.e. 10.688 eV [17], 9.677 eV [4] and 9.40 eV calculated in the present work.

Declaration of Competing Interest

The authors declare that they have no known competing financial interests or personal relationships that could have appeared to influence the work reported in this paper.

CRediT authorship contribution statement

R. Locht: Conceptualization, Investigation, Validation, Resources, Data curation, Writing – original draft, Funding acquisition. **D. Dehareng:** Methodology, Software, Formal analysis, Data curation, Funding acquisition.

Data availability

No data was used for the research described in the article.

Acknowledgments

R.L. gratefully acknowledges the European Community for its support through its I3 (Contract R II 3 CT-2004-506008). D.D.'s contribution was supported by the Belgian program on Interuniversity Attraction Poles of the Belgian Science Policy (IAP n° P6/19).

Supplementary materials

Supplementary material associated with this article can be found, in the online version, at doi:10.1016/j.jqsrt.2023.108640.

References

[1] McLinden MO, Kazakov AF, Brown JS, Domanski PA. Int J Refrigeration 2014;38:80.
[2] Theimer R, Nielsen JR. J Chem Phys 1957;26:1374.
[3] Hoxha A, Locht R, Leyh B, Dehareng D, Hottmann K, Jochims HW, Baumgärtel H. Chem Phys 2000;260:237.
[4] Locht R, Dehareng D. J Quant Spect Rad Trans 2023;305:108626.
[5] Locht R, Dehareng D, Leyh B. AIP Adv 2019;9:015305.
[6] Locht R, Dehareng D, Leyh B. J Quant Spect Rad Trans 2020;251:107048.
[7] (a) Marmet P. Rev Sci Instrum 1979;50:79; (b) Carbonneau R, Bolduc E, Marmet P. Can J Phys 1973;51:505; (c) Carbonneau R, Marmet P. Can J Phys 1973;51:2203; (d) ibid. Phys Rev 1974;A 9:1898.
[8] Lofthus A, Krupenie PH. J Phys Chem Ref Data 1977;6:113.
[9] (a) Tiesinga E, Mohr PJ, Newell DB, Taylor BN. J Phys Chem Ref Data 2021;50:033105; (b) Mohr PJ, Newell DB, Taylor BN. Rev Mod Phys 2016;88:035009.
[10] Frisch MJ, Trucks GW, Schlegel HB, Scuseria GEMA, Robb MA, Cheeseman JR, Scalmani G, Barone V, Mennucci B, Petersson GA, Nakatsuji H, Caricato M, Li X, Hratchian HP, Izmaylov AF, Bloino J, Zheng G, Sonnenberg JL, Hada M, Ehara M, Toyota K, Fukuda R, Hasegawa J, Ishida M, Nakajima T, Honda Y, Kitao O, Nakai H, Vreven Montgomery JA Jr., Peralta JE, Ogliaro F, Bearpark M, Heyd JJ, Brothers E, Kudin KN, Staroverov VN, Kobayashi R, Normand J, Raghavachari K, Rendell A, Burant JC, Iyengar SS, Tomasi J, Cossi M, Rega N, Millam JM, Klene M, Knox JE, Cross JB, Bakken V, Adamo C, Jaramillo J, Gomperts R, Stratmann RE, Yazyev O, Austin AJ, Cammi R, Pomelli C, Ochterski JW, Martin RL, Morokuma K, Zakrzewski VG, Voth GA, Salvador P, Dannenberg JJ, Dapprich S, Daniels AD, Farkas O, Foresman JB, Ortiz JV, Cioslowski J, Fox DJ. *Gaussian 09*, revision A.02. Wallingford CT: Gaussian, Inc; 2009.
[11] Dunning TH Jr.. J Chem Phys 1989;90:1007.
[12] Zhao Y, Truhlar DG. Theor Chem Acc 2008;120:215.
[13] Van Caillie C, Amos RD. Chem Phys Lett 2000;317:159.
[14] (a) Robin M.B., *Higher excited states of polyatomic molecules,* Vol. I pp 51 (1974); (b) ibid. Vol.II pp 50 (1975), Academic Press, New York.
[15] Herzberg G. Molecular spectra and molecular structure. III. electronic spectra and electronic structure of polyatomic molecules, 67. Princeton, N.J.: D. Van Nostrand Co. Inc.; 1967.
[16] Locht R, Jochims HW, Leyh B. Chem Phys 2012;405:124.
[17] Locht R, Dehareng D, Leyh B. J Phys B At Mol Opt Phys 2012;45:115101.